MIXIQ: Re-thinking Ultra-low Power Receiver Design for Next-generation On-body Applications

Mohammad Rostami[1], Xingda Chen[1], Yuda Feng[1], Karthikeyan Sundaresan[2], and Deepak Ganesan[1]
[1]University of Massachusetts Amherst
[2]NEC Labs of America

ABSTRACT

A long-standing challenge in radios for wearables is to design ultra-low power, yet high performance receivers with good sensitivity and spectral efficiency while being compatible with WiFi. The vanilla envelope detector used in standard UHF RFID is the most popular receivers on backscatter tags since they are passive but suffer from poor sensitivity and cannot decode complex modulations, which makes them a poor choice for directly decoding data from WiFi packets.

In this paper, we present the design of an easy-to-prototype ultra-low power WiFi receiver called MIXIQ that operates at μWs of power while providing improved sensitivity and decode-ability of complex high-rate signals. MIXIQ uses the signaling capabilities of the newest standard of WiFi, 802.11ax, to turn a standard WiFi packet into a helper + data signal. The same non-linear RF circuit used in a vanilla envelope detector, when driven by this twin signal, now behaves like a *passive mixer* i.e. it down-converts the RF carrier data to the sub-MHz range without adding any energy overhead. MIXIQ then uses an ultra low-power largely digital baseband pipeline to (i) significantly boost sensitivity using ultra low power components; (ii) enable the demodulation of complex signals for substantial boost in spectral efficiency. We show that MIXIQ improves upon the vanilla envelope detector by 25dB in sensitivity and 89× in bandwidth efficiency, while consuming 0.3mW for a PCB-based implementation and 40μW for CMOS simulation. We also demonstrate a Hearable system that leverages MIXIQ to improve VOIP reception range by 10× compared to a vanilla envelope detector.

1 INTRODUCTION

A significant body of research in wireless communication in recent years has focused on the development of ultra-low power backscatter radios that can operate on extremely tiny power budgets while being compatible with commodity radios such as WiFi, LoRa, BLE and Zigbee [5, 13, 14, 16, 24, 35, 53, 57]. Of these, WiFi compatibility is perhaps the most important given the widespread coverage offered by WiFi. An efficient and reliable WiFi backscatter system can be a key cog on how we design IoT and wearables, particularly when high data rates are needed.

ACM MobiCom '21, January 31-February 4, 2022, New Orleans, LA, USA

ACM ISBN 978-1-4503-8342-4/22/01…$15.00
https://doi.org/10.1145/3447993.3483270

The majority of these efforts, however, focus on enhancing upstream communication from the tag to the application device with few, if any, hardware-level enhancements to the tag-side receiver for downstream communication. For example, while the WiFi backscatter uplink has evolved over the years to achieve impressive bitrates of >10 Mbps (e.g. [58]), downlink performance has largely remained stagnant. Most WiFi Backscatter efforts use the same *vanilla* envelope detector (Vanilla-ED) circuit that is used in standard UHF RFID (figure 1) on the tag PCB with off-the-shelf parts, and reverse-engineer the WiFi packet to mimic an OOK signal that is decodable by the detector. However, this OOK emulation is inefficient and has poor spectral efficiency (throughput in the low 100s of Kbps) [13].

The upstream communication advances in backscatter have relied on easy-to-prototype elements like RF switches, transistors, and simple circuits. As a result much of the recent systems activity in backscatter has focused on the upstream communication with limited enhancements to the receiver.

This gap has skewed exploration of new research and application ideas within backscatter communication. While several efforts have focused on leveraging the growing uplink bandwidth of WiFi backscatter to transmit richer sensor data to the base station, for example, streaming video and audio in real-time [20, 36], there has been essentially no work on applications like Hearables that are dominated by downlink data transfer [4, 6, 8, 49]. Similarly, work on Backscatter MAC and upper layers have been skewed by the fact that the downlink is highly inefficient.

To fill this gap, we introduce MIXIQ , a novel ultra low power receiver design that (i) greatly outperforms the Vanilla-ED used in most backscatter tags, (ii) can be easily prototyped with off-the-shelf components, and (iii) is compatible with WiFi to enable an easy-to-deploy high throughput downlink that leverages OFDMA. MIXIQ adopts two strategies to fulfill these goals:

(1) Sub-carrier based WiFi packet emulation: The key contribution of our work is an OFDMA-compatible sub-carrier based (rather than symbol based) WiFi packet emulation technique that retains the benefits of using an envelope detector while (a) allowing the transmitter to use its full dynamic range of power and (b) allowing the use of bits of data encoded in individual subcarriers. This technique is based on the fact that when an envelope detector receives two carriers, a data-carrying signal intertwined with a "helper" signal without data, at separate frequencies, it will behave like a frequency mixer and output a signal delta between the pair of transmitted signals which has the same phase and amplitude as the input data signal. Thus, the MIXIQ receiver can down-convert the data signal from UHF frequencies (e.g. 2.4GHz) to a LF (few 100 KHz) delta signal, all while preserving the complex phase and amplitude of the high data-rate data signal without any additional energy cost.

Our ideas extend those that have been proposed in prior work; for example, several backscatter systems leverage envelope detector non-linearity for creating an external helper tone [17, 45] and some work has looked at creating two identical tones from an OFDMA transmitter [30]. We combine these building blocks in the context of a receiver design, but also enhance them by showing that we can leverage the fine-grained frequency resolution offered by OFDMA versions (802.11ax, WiFi 6) to transmit two different signals from a WiFi transmitter (helper and data). This allows MIXIQ to be deployed with commodity WiFi radios that support 802.11ax.

(2) Digital-heavy demodulation pipeline: In addition to optimizing RF down-conversion, we also need to avoid the use of power-hungry RF/analog components in the demodulation pipeline to operate at the desired μW power regime while being able to decode complex, high data-rate signals.

To address this, MIXIQ employs an extremely power efficient, largely digital implementation of the entire demodulation pipeline. While such a digital-heavy approach is typically less power-efficient compared to analog, MIXIQ leverages the fact that the externally-assisted down-conversion results in very low frequencies (LF) of 100s of KHz. This in turn, paves the way for several optimizations: (i) *high-impedance voltage amplification* that substantially improves sensitivity with minimal additional energy cost (unlike power amplification) since MIXIQ can take advantage of the LF signal to leverage high impedance components at both the input and output (power $\propto V^2/Z$); (ii) *high resolution ADC* that preserves information of high data rate signals while consuming very little power owing to the low sampling rate (1 MSPS) for the LF signal; and (iii) *full-digital IQ demodulation* by correlating with sampled sine and cosine signals entirely with digital circuits, thereby completely eliminating the need for analog filtering and its associated degradation in analog demodulators, while requiring significantly lower power. This also provides robustness to interference by considering the latter as noise in the digital domain.

Performance: We have implemented all different parts of MIXIQ using commercial off-the-shelf devices and components. On the WiFi TX side, we use a commercial WiFi 6 device (Qualcomm IPQ6010 [27]) and a version of openWRT driver on top of it to implement the sub-carrier based emulation. In addition, we prototyped MIXIQ's receiver on PCBs and have comprehensively characterized its performance and power consumption under various conditions.

Our evaluations reveal that MIXIQ delivers a WiFi decoding sensitivity of -55dBm and a spectral efficiency of 0.51 bps/Hz (1.125 Mbps over 2.2 MHz bandwidth), which substantially improves upon Vanilla-ED by 25dB and 89×, respectively. Further, our case study with a Hearable system built with MIXIQ as its receiver, reveals that it can receive high-rate VOIP data from a WiFi device with good signal quality and 10× the operational range of a Vanilla-ED. We believe MIXIQ's contributions can open the door for higher performance ultra-low power receivers to be integrated with backscatter transmitters in several new and compelling applications in body area networks.

2 LIMITATIONS OF VANILLA-ED AS WIFI RX

In this section, we discuss in more depth why much of the recent experimental on backscatter communication still rely on Vanilla-ED circuit as their receiver despite the fact that it delivers very poor performance.

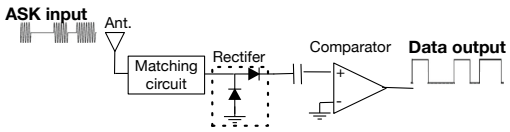

Figure 1: Block diagram of Vanilla-ED.

A Vanilla-ED consists of an RF rectifier circuit (typically based on a Schottky diode) followed by an ultra low power voltage comparator, figure 1. When an OOK signal arrives at the antenna, the rectifier converts the RF signal to an amplitude-varying LF signal. The comparator then generates 0s and 1s based on whether the amplitude is below or above the threshold. Such a circuit is very energy efficient and also easy to assemble using one of the many RF Schottky diodes and ultra low power comparators in the market.

The Vanilla-ED is also simple to interface with WiFi by manipulating the payload of a packet to mimic an OOK signal (e.g. [13]). This makes it possible for Vanilla-ED on a backscatter tag to directly decode the conveyed data bits within a standard WiFi packet.

The downside of using Vanilla-ED as a receiver, however, is that sensitivity is only around -20dBm to -30dBm when prototyped using off-the-shelf components, regardless of the bit rate. This makes it impractical for many interesting application scenarios for ultra-low power communication. For example, on-body links (e.g. from wrist to head) can easily introduce up to 60dB attenuation to the transmit signal at practical distances [33, 52]. Hence, if the transmitting device (say, a smartwatch) operates at 10dBm, the RSSI can be as low as -50dBm, which is far below the sensitivity of the detector. In addition, since the envelope detector is only sensitive to the power (i.e. amplitude) of the received RF signal, it has poor spectral efficiency. The entire band needs to be free during the time the tag is receiving data from the transmitter and no more than one bit can be sent to the tag during each symbol time.

When the Vanilla-ED is used for WiFi reception, performance is further diminished for three reasons. First, the TX power of WiFi TX is at least 10 dB lower than the radiated power of an RFID reader which means that range is severely limited. Second, the dynamic range of the emulated OOK signal via manipulating WiFi packets (i.e. the difference between low an high power levels) is also several dBs lower compared to the genuine OOK signal that is output by RFID TX antenna. Third, WiFi operates at 2.4GHz rather than 900MHz which suffers from more channel attenuation. As a result, the simplicity of the Vanilla-ED also comes with significant downsides.

3 OVERVIEW OF MIXIQ

We present MIXIQ – a new ultra low power WiFi receiver design that is easy to prototype using off-the-shelf components. MIXIQ transforms the passive envelope detector to behave like an advanced receiver with high sensitivity and ability to decode complex, high data rate signals, while also keeping its energy footprint in the μW regime even when it is implemented with off-the-shelf components. MIXIQ is built on two techniques, as shown in figure 2.

1. Transforming the RF rectifier into an externally triggered passive mixer: The first contribution in MIXIQ is a technique to

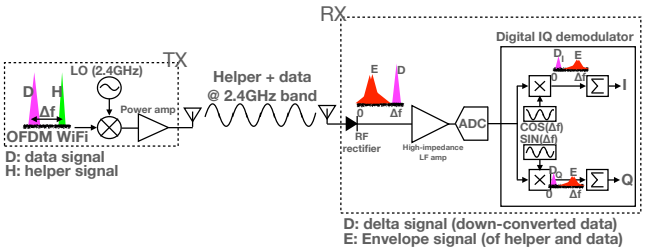

Figure 2: Overview of MIXIQ .

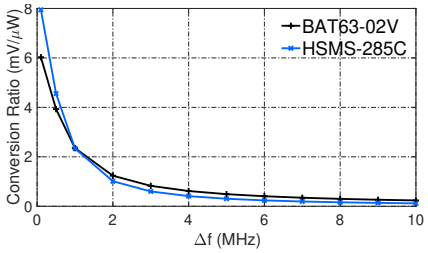

Figure 3: Conversion ratio of RF rectifiers vs. Δf.

enable a "helper tone" signal to be provided *externally* by the transmitting WiFi device, allowing us to offload its energy requirement from the receiver to the transmitter. The helper tone signal is needed as input to a mixer which multiplies (or mixes) with the incoming data RF signal – the output has an intermediate frequency (Δf) of $f_{data} - f_{helper}$ which is a down-conversion of the incoming RF frequency.

To reduce the power consumption of the mixer, MIXIQ generates a helper signal by employing a new signaling approach whereby the data-carrying signal is accompanied by a "helper" signal (without any data) at a slightly different frequency as shown in figure 2.

The helper signal is intelligently designed such that it can be seamlessly embedded alongside the data signal into existing WiFi signal waveforms, making MIXIQ compatible with commodity WiFi devices. When such a *helper+data* signal passes through an envelope detector, the latter's non-linearity allows for the conversion of the incoming data signal to a much lower frequency that is the difference of the two carrier frequencies (called *delta* signal). Thus, the information (phase and amplitude) from the incoming UHF data signal (e.g. 2.4 GHz) is transferred onto the delta signal at just a few hundred KHz, without any additional energy cost. If we denote the incoming UHF data and helper signals by $X_d(t) = A_d(t)\cos(2\pi f_d t + \phi_d(t))$ and $X_h(t) = A_h\cos(2\pi f_h t)$, then the rectifier's output is:

$$V_{rect.} = A_d^2(t) + A_h^2 + 2A_hA_d(t)\cos(2\pi\Delta f t + \phi_d(t)) \quad (1)$$

The last term is the resulting delta signal at Δf that preserves the amplitude and phase of the incoming UHF data signal.

We note that prior work has also used a helper tone [18] to turn an envelope detector into an externally-triggered passive mixer but the difference is that this effort used a separate "helper" device that emits a pure tone helper signal whereas MIXIQ uses the capabilities of OFDMA WiFi to embed the helper signal within the same device that is sending the data signal. Thus, our approach is more practical in terms of deployability.

2. An ultra low power digital-heavy demodulation pipeline: The delta signal (with frequency Δf) at the output of the mixer, is accompanied by some inter-modulation terms that arise due to the re-purposed rectifier not being an ideal mixer. In other words, it outputs the envelopes of the data and helper signals, which can interfere with the down-converted delta signal. MIXIQ leverages the very low frequency nature of the delta signal to design a highly power-efficient demodulation pipeline that not only gets rid of the undesired inter-modulation signals, but also increases (a) sensitivity through voltage amplification that leverages high impedance analog components at micro-power, and (b) spectral efficiency through a fully-digital micro-power IQ demodulation (Figure 2) that eliminates the degradation faced by the analog demodulators.

3.1 Practical Challenges

Realizing MIXIQ's architecture in practice necessitates addressing several technical challenges.

Challenge 1: Embedding data + helper signal in WiFi packets: The helper signal needs to be generated in the same commodity device that is sending the data signal since a separate device for helper signal generation makes the system less practical. Further, the helper and data signals should be sufficiently separated in the frequency domain, with the spectrum between them being unused so that the delta signal is created at the envelope detector.

Challenge 2: Tradeoff between bandwidth and sensitivity: Increasing the channel bandwidth contributes to larger data rates but results in a severe degradation of receive sensitivity. Higher bandwidth requires a higher Δf; however, increasing Δf has two detrimental effects on sensitivity: (1) the downconversion ratio i.e. the ratio between the amplitude of the downconverted signal at the output of the rectifier and RF input power, rapidly decreases with higher Δf as shown in Figure 3 for two different RF rectifiers (BAT63-02V [12], and HSMS-285C [3]), indicating the generality of the problem; (2) gains achieved by micro-power amplifiers at higher Δf are lower. For example, for a bandwidth of 1 MHz, we need a Δf of several MHz (e.g. 8MHz in [25]), to be able to filter out the unwanted low-frequency terms as well as perform IQ demodulation successfully. However, as shown in Figure 3, the down-conversion ratio is less than 0.3mV/μW, which contributes to around 15dB worse sensitivity, compared to when the bandwidth is as low as 100 KHz. Further, the state of the art designs do not achieve more than 30dB voltage gain with micro-power amplifiers at these frequencies, compared to the 60dB voltage gain possible at sub-MHz frequencies, thereby leading to another 15 dB difference in sensitivity. Thus, migrating from sub-MHz to several MHz for obtaining higher bandwidth can compromise the sensitivity by as much as 30dB.

Challenge 3: Preserving the amplitude and phase information accurately: Demodulation of complex waveforms requires us to track the abrupt changes in the amplitude and phase of the down-converted data signal without introducing any distortion. However, achieving this goal with passive and low power components is challenging. Consider a passive RLC filter that is used to eliminate the unwanted low frequency components at the output of the rectifier. If it has a wide passband, it cannot completely filter out the unwanted terms that are very close in frequency to the down-converted data signal. On the other hand, a narrow passband makes the filter simple but unable to track the rapid changes in amplitude

and phase, rendering it not useful for IQ demodulation. In essence, designing a base-band for our receiver is highly non-trivial.

Challenge 4: The impact of interference: Even though MIXIQ's design behaves like an active radio in many aspects, it is still frequency non-selective like an envelope detector, i.e. it is unable to distinguish the frequency of the RF signal received at the antenna. Hence, if there exists another signal at frequency f_i, $X_i(t) = A_i(t)\cos(2\pi f_i t + \phi_i(t))$in Equation1, it will also be detected by the rectifier, with the corresponding low frequency term A_i^2 appearing at the output. Also, other terms such as $2A_hA_i(t)\cos(2\pi(f_i - f_h)t + \phi_i(t))$ and $2A_d(t)A_i(t)\cos(2\pi(f_i - f_d)t + \phi_i(t) - \phi_d(t))$ might also appear close or even overlap with the *delta* signal in the frequency domain. These terms interfere with the down-converted data signal, affecting its demodulation. We also wish to avoid deactivating other transmitters in the network during MIXIQ's reception since this will hurt spectral efficiency as only a small fraction of the entire band (e.g. only hundreds of kHz of the total 80MHz of the 2.4GHz ISM band) will be used.

We now present MIXIQ's design components that tackle these challenges.

4 EXTERNAL DOWN-CONVERSION WITH COMMODITY RADIOS

MIXIQ enables commercial WiFi 6 devices to transmit a *helper + data signal* with no hardware modifications and also no change in the format of standard 802.11ax packets.

4.1 Leveraging Spectrum Channelization

To account for the tradeoff between larger bandwidths (hence larger Δf) and lower sensitivity, MIXIQ leverages 802.11ax's OFDMA to operate commodity transmissions on much smaller bandwidths (2.2MHz). This allows it to design the LO signal with a much smaller Δf and has three key benefits. The first is increased sensitivity from improved down-conversion ratio and ultra low power amplifier gains (discussed in Section 3.1). The second is increased data rates from sampling the down-converted signal at a higher resolution, allowing for a fully digital IQ demodulation of complex, high-rate modulations at ultra low power consumption (discussed in Section 5.3). The third is increased spectral efficiency from not only increased data rates on individual transmissions but the ability to multiplex multiple such transmissions from different users on orthogonal spectral chunks (called resource units, RUs). A resource unit can be as small as 2.2MHz (i.e. $\frac{1}{10}\times$ 22 MHz channel bandwidth). Hence, the LO signal would occupy only 2.2MHz of the WiFi channel, while the rest of the RUs can be allocated to other WiFi (either MIXIQ or legacy) transmissions. Note that such a multiplexing is not possible with existing passive receiver designs, where the energy on the entire bandwidth (WiFi transmission) is used to decode low-rate information.

4.2 Placement of the LO Signal

OFDMA allows for splitting a given bandwidth into several smaller sub-channels (RUs), each consisting of a set of sub-carriers that can be individually modulated. MIXIQ leverages this feature to embed the data and helper signals within a single RU, where each

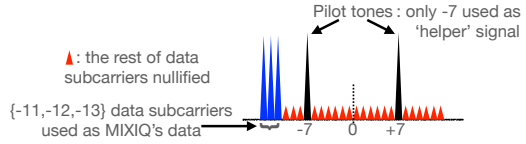

Figure 4: MIXIQ 's signaling within a 802.11ax RU.

of the signals occupy one or more sub-carriers and are separated by several sub-carriers in between, as shown in Figure 4.

Selecting Δf: In order to successfully demodulate the down-converted IQ data signal, the symbol rate must be sufficiently smaller than the carrier frequency. The output of the IQ demodulator contains the original I and Q values along with some residual terms – a larger magnitude of the latter leads to demodulation errors. If we denote the delta signal as: $r(t) = i\cos(2\pi\Delta f t) + q\cos(2\pi\Delta f t)$, where i and q are called the in-phase and quadrature parts of the signal, the obtained I and Q values in digital domain can be written as: $\hat{I} = \frac{1}{k}\sum_1^k r(nT).\cos(2\pi\Delta f nT)$ and $\hat{Q} = \frac{1}{k}\sum_1^k r(nT).\sin(2\pi\Delta f nT)$. ($T$ is the sampling period). The ratio between the magnitude of the residual terms, (i.e. the difference between $\hat{I}$, $\hat{Q}$ with the original i and q) and the magnitude of the constellation points reduces as $\Delta f \times T_S$ (where $T_S = k.T$ is the symbol time) increases. Numerical analysis on the residual terms show that when $\Delta f \times T_S \leq 3$, the value of $\hat{I} + j\hat{Q}$ falls into other constellation points, resulting in demodulation error. Therefore, $\Delta f \times T_S > 3$ is necessary for enabling high order modulations that need a larger ratio (e.g. 25dB for QAM-64).

Selecting helper and data signals: MIXIQ leverages the smallest RU of 2.2 MHz, which consists of two pilot tones (sub-carriers). Given that the pilot tones cannot be suppressed, MIXIQ employs one of the pilot tones (-7) as its helper signal, as shown in Figure 4. With the chosen Δf > 234kHz, the sub-carriers used for carrying the data signal in our transmitter should be at least 4 sub-carriers away from the helper signal. There are 18 such data subcarriers in our 2.2MHz RU (all of them except {-10,-9,-8,-6,-5,-4}).

MIXIQ uses only the three sub-carriers on the left side of the {-7} pilot tone, i.e. {-13,-12,-11}. The reason is that the rest of the subcarriers located on the right side of the {-7} pilot tone, i.e. {-3,-2,...,+12,+13} either overlap in frequency with {-13,-12,-11} after the passive mixer, or are too far from the {-7} helper tone which in turn degrades sensitivity. Δf does not exceed 468.75kHz for any of the chosen data sub-carriers, and remains in the efficient region of sub-MHz, wherein both the down-conversion ratio of the rectifier and the gains of the micro-power voltage amplifiers are high. This enhances sensitivity of our receiver.

Choosing Δf to be less than 468.75kHz also ensures that the bandwidth of the data signal after down-conversion does not exceed 500kHz; hence, its information will be fully preserved when being sampled at 1MSPS (1MSPS > 2 × 500kHz ; Nyquist theorem). This allows MIXIQ to leverage extremely low power, very high resolution (e.g. 12-bit) ADCs at the desired 1MSPS sampling rate, which are available both off-the-shelf [40] and as ASIC [43]. Thus, the data signal can be transferred to the digital domain, where demodulation can be accomplished using ultra low power logic elements without compromising accuracy, which reduces power consumption.

Nullifying unwanted data sub-carriers: Sub-carriers not used for the data and helper signals need to be nullified to prevent corruption of the LO signal that is needed for accurate down-conversion. While one cannot completely nullify a sub-carrier, MIXIQ leverages higher-order modulations to "almost" nullify un-wanted sub-carriers – the farthest constellation points in higher-order modulations (e.g. QAM-256) from the origin can have more than 15× greater amplitude than the closest ones. Thus, data and helper sub-carriers are assigned constellation points with the largest magnitude, while others are nullified by assigning those with the smallest amplitude.

Minimizing the residual terms that appear as transmitter noise: The fact that unwanted sub-carriers do not become completely nullified does, however, impact noise. Although the unwanted sub-carriers get the constellation points with the lowest power to resemble nullified sub-carriers, these small values can add up and appear as a significant *transmitter noise* term. The noise power is at its peak when the *low amplitude* constellation points assigned to the nullified sub-carriers have all the same phase resulting in a constructive total sum.

To address this problem, we search for the combination of the phases for the unwanted sub-carriers (through exhaustive search) that minimizes their impact. This is a one-time effort and after 162 iterations of the search, MIXIQ is able to reduce the power of these residual terms after demodulation to be 35dB below at the power of the data for every down-converted data sub-carrier. This ratio is well above the ratio required for successful demodulation of QAM-64 signals (25dB).

Compliance with 802.11ax standard: Our signaling method also complies with the packet structure defined in 802.11ax standard. When the WiFi TX device is sending the "data+helper" signal as we have proposed, it is actually sending packets in its normal mode of operation. As a result, our approach does not impact any aspect of the performance, including the power consumption, of the WiFi TX device. Additionally, the WiFi TX device operates as a normal WiFi 802.11ax-compatible client of a 802.11ax WiFi network: it takes a portion of the channel that is assigned by the WiFi AP, called resource unit (RU), to transmit the data + helper signal. Since RUs are separated in frequency domain, it will not interfere with other WiFi clients that take different RUs for transmitting their packets to the AP.

4.3 Encoding the Data Signal

Once the data subcarriers in the RU are selected, MIXIQ optimizes their modulation and coding to ensure a robust delivery of high-rate modulations.

Modulation scheme selection: While the highest modulation order available in 802.11ax is QAM-1024, which translates to 10 bits per subcarrier per symbol time, MIXIQ employs QAM-64 that has six bits per subcarrier per symbol time. Modulations higher than QAM-64 are less robust to the residual terms of the IQ demodulation, and fail to work with the closest data sub-carriers (and hence Δf) chosen. On the other hand, incorporating an additional data subcarrier or increasing Δf to accommodate even higher modulations, impacts the power consumption and sensitivity of the receiver. Hence, MIXIQ settles for QAM-64 to maintain the optimal design choice of the data-subcarriers. MIXIQ 's design choices result in a raw throughput of: 3 subcarriers $\times$ 6 $\frac{\text{bit}}{\text{subcarrier}} \times \frac{1}{16\mu s}$ = 1.125Mbps over the 2.2 MHz RU.

LDPC for coding: MIXIQ leverages the option of LDPC (low density parity check) codes in 802.11ax (compared to convolutional codes in prior standards). Being a type of block codes, LDPC allows for better control of the data in different RUs, since the data bits are separated from the parity bits, unlike convolutional codes, where they are interleaved. Also, the scrambler before the LDPC can be easily reverse engineered given its known pattern.

4.4 Reverse-engineering 802.11ax

Finally, we need to reverse-engineer the 802.11ax pipeline to determine the appropriate payload bits that will generate the desired data and helper waveform $Y(t)$. We borrow the 802.11ax reverse engineering technique introduced in [30], but with two main differences. First, [30] nullifies all the data sub-carriers in the 26-tone resource unit and only keeps the two pilot tones as the twin-carrier signal; whereas, we want to use data sub-carriers {-13,-12,-11} for data transmission. Second, the twin carrier signal emulated in [30] is sensitive cyclic prefix wherein a small chunk of the initial samples that is added to the tail of the 256-element vector of IQ samples. Therefore, their choice is limited to 8-th resource unit. However, MIXIQ receiver can completely ignore the cyclic prefix part and focus on the main 256-element vector when demodulating and thus the cyclic prefix step of the reverse engineering can be skipped. As a result, MIXIQ can leverage any 26-tone RU within the channel which is beneficial when co-existing with other devices in the WiFi network.

Therefore, we take the following steps for reverse engineering the payload of the standard 802.11ax packets in uplink trigger mode when the client is sending on a 26-tone resource unit.

FFT: The OFDMA modulator of 802.11ax takes a 26-element complex vector, $Y_{FFT}(f)$ as input and performs inverse fast fourier transform (IFFT) to obtain the transmit signal in time domain. Each element of $Y_{FFT}(f)$ corresponds to the phase and amplitude of one of the 26 subcarriers (24 data subcarrier and two pilot tones) within the resource unit. The output of IFFT, $Y_T(t)$ is a 256-element complex vector that determines the I and Q values. Note that in OFDMA all the sub-carriers outside the selected resource unit are null. Since FFT and IFFT are inverse mathematical functions, we can calculate $Y_{FFT}(f)$ by taking the FFT of $Y_T(t)$ as,

$$Y_{FFT}(f_m) = \sum_{n=1}^{256} Y_T(n)\, e^{-j2\pi f_m n}, \tag{2}$$

where f_m is the frequency of a sub-carrier in the selected RU.

QAM-64 constellation de-map: In our configuration of the 802.11ax device, every element of Y_{FFT} is assigned to a QAM-64 constellation point. Since our goal is to nullify all of the data subcarriers except {-13,-12,-11}, we select the constellation points with the lowest energy, or closest ones to the origin, for those subcarriers. Note that the two pilot tones cannot be reverse engineered and they toggle between +1+0j and -1+0j per OFDM symbol according to the pattern specified in 802.11ax standard. In QAM-64, the closest points to the origin are $C_1 = 0.17 + 0.17j$, $C_2 = 0.17 - 0.17j$, $C_3 = -0.17 - 0.17j$, and $C_4 = -0.17 + 0.17j$. Thus, every 6-bit chunk

of Y_{DM} for data sub-carriers {-10,-9,-8,-6...,+6,+8,+12,+13} maps to a complex number from the set $\{C_1, C_2, C_3, C_4\}$.

LDPC decode: Next, we need to find the data bits that result in the desired constellation points. The 802.11ax standard is equipped with an LDPC encoder that converts the input bit-vector Y_{DC} consisting of the bits of the data to the encoded bit-vector Y_{DM} and then every 6-bit sector of Y_{DM} is converted to a QAM-64 constellation point. Y_{DM} is obtained by attaching parity bits to chucks of Y_{DC}, which can be shown as $Y_{DM}^{(i)} = Y_{DC}^{(i)}.H$ where H is the matrix of the code [15]. The size of the data chunks followed by parity blocks is determined by LDPC code rate. We choose the highest rate = $\frac{5}{6}$ to maximize the throughput since it minimizes the size of parity blocks that cannot be reverse engineered. In this case, the 802.11ax LDPC encoder takes every 12000-bit chunk of data bits, $Y_{DC}^{(i)}$ and attaches a 2400-bit chunk of parity bits to obtain $Y_{DM}^{(i)}$.

De-scramble: Finally, we perform the inverse of the scrambling that is done on the input data bits before they are LDPC encoded. This is straightforward since the 802.11ax scrambler consists of a linear-feedback shift register (LFSR) and the initial state of the LFSR is known from the standard. Therefore, we can reverse the steps from the desired data bits to the initial bits of the LFSR to find the input data bits.

5 RECEIVER ARCHITECTURE

We now describe MIXIQ 's receiver baseband pipeline that is employed at the output of the rectifier. Our goal is to achieve the desired sensitivity and spectral efficiency at μW by leveraging MIXIQ 's choice of subcarriers which results in a small Δf (described in 4.2).

5.1 High-impedance voltage amplification

At UHF radio frequencies such as 2.4GHz, it is important to keep input and output impedance of the amplifiers at 50Ω to avoid reflection loss caused by impedance mismatch. In contrast, at sub-MHz frequencies, one can have stable voltage amplifiers with input and output impedance much greater than 50Ω (e.g. tens of kΩ), while providing up to 60dB voltage gain. Being high-impedance at the input and output reduces the power dissipation of these amplifiers to μW levels. Hence, SNR can be dramatically increased, which improves the sensitivity even for high-order modulations that need high SNR (e.g. 25dB for QAM-64) for successful demodulation.

5.1.1 Two-stage common-emitter based amplification: MIXIQ employs a voltage amplifier design, consisting of a few common-emitter (in BJT implementation, or common-sources in our CMOS simulations which we discuss later) stages that can significantly amplify the output of the rectifier at μW power consumption, with a minimal distortion to amplitude and phase of the down-converted data signal. Figure 5 shows an implementation of a micro-power amplifier with NPN bipolar junction transistors (BJT). It consists of two stages for generating a higher voltage gain. The NPN transistor used at each stage is an On Semiconductor 2N3904 [22], which is biased using these values: $R_{B_1} = R_{B_2} = 10k\Omega$, $R_C = 9.1k\Omega$, $R_E = 2.2k\Omega$, and $C_B = C_E = C_C = 100nF$ ($V_{cc} = 1.8$v).

Voltage gain: Each stage of our implemented BJT amplifier has 33.0dB small signal (SS) gain. However, this happens only when it is not impacted by the input and output load impedances. In practice, the voltage at the output of the first and second stages get compromised by about 3dB each because of the loading effect at their input and output. Thus, the overall gain of MIXIQ's two-stage amplifier is about 57dB when the amplifier is placed between the rectifier and the next stage in the pipeline.

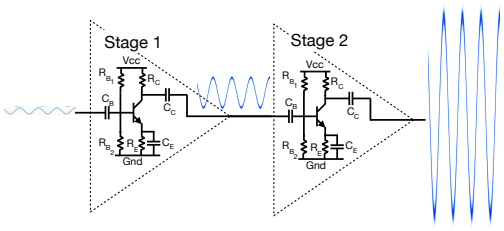

Figure 5: Two-stage common-emitter amplifier.

5.1.2 Distortion control: Employing high impedance pushes the bias point of the transistors very close to the saturation region of the transistor. Hence, if the output of the rectifier, is greater in amplitude, the transistors can saturate, severely distorting the amplitude and phase of the down-converted data signal. To overcome this issue, MIXIQ employs a gain control unit that measures the received signal strength (RSS), based on which it decides to turn off the amplifier either fully or partially if necessary to prevent distortion of the down-converted data signal.

MIXIQ allocates the first two symbols of the WiFi packet are for RSSI measurements based on which the receiver decides how many stages to be used for the rest of the packet that contains actual data bits. Therefore, MIXIQ performs the distortion control with no additional components. Note that this reduces the overall throughput but if the channel variations are not so fast it can be reduced to one channel control per ten packets thereby minimizing its overhead.

5.2 Low-power ADC

The output of the rectifier is just a few hundreds of kHz, which allows MIXIQ to acquire the whole delta waveform with just a sampling rate of 1MSPS (1 Mega samples per second). Thus, a reasonably high-resolution (12-bit) ADC can be employed to convert the signal to the digital domain at very low power, thereby paving the way for full-digital IQ demodulation. Note that MIXIQ provisions a buffer (common-collector in BJT, or common-drain in CMOS) stage between the output of the amplifier's second stage and ADC's input to minimize the impact of ADC's low input impedance (2.5kΩ). Therefore, the overall gain is compromised by only 6.1dB; as opposed to 16.9dB if there were no buffer between amplifiers and ADC.

5.3 Fully-digital IQ demodulation

Demodulation of complex signals such as QAM-64 requires an IQ demodulator that does not influence the amplitude and phase of the delta signal. Briefly, an IQ demodulator calculates the correlation of the incoming modulated signal with the cosine and sine waveforms to obtain the in-phase (I) and quadrature (Q) component values, respectively. Then, the closest constellation point to the

calculated I+jQ value (after scaling the amplitude) is determined so as to decode the data bits.

Challenges with analog implementation: One challenge is that analog components used to implement the correlation (e.g. analog multipliers), are non-ideal and produce unwanted terms such as the square terms of the inputs. Thus, if the low frequency terms, i.e. the envelopes of the data and helper, are not filtered out, the comparator will produce their inter-modulation, which will interfere with the output of the correlator. Hence, there needs to be an analog filter between the rectifier and the analog IQ demodulator. However, using analog filters leads to a degradation in sensitivity and/or throughput, as discussed in §3.1.

Full-digital design: Figure 2 shows the building blocks of MIXIQ's IQ demodulator, which consists of all the tasks, including the multiplications, being implemented arithmetically with digital circuits. This in turn, prevents the inter-modulations, thereby allowing it to completely bypass the bandpass filter in its design.

In essence, MIXIQ digitally multiples the samples of the delta signal with the locally stored cosine and sine waveforms. The different values of the cosine and sine waveforms at different timestamps are stored in permanent memory for instantaneous access at the same sampling rate at which the delta signal is acquired.

The digital multiplication is implemented with in a parallel way and therefore the clock frequency of the demodulator logic circuit does not have to be several times higher than ADC sampling rate. In addition, we use an ultra low power CPLD (complex programmable logic device) for implementing the logic. CPLDs are very similar in nature to FPGAs – both programmable logic – but can be found at lower energy footprints than FPGAs since they have less complex logic blocks and resources than FPGAs. Therefore, a CPLD that works at low clock frequency substantially reduces the power consumed during demodulation.

Robustness Against Interference: Since the rectifier cannot distinguish the frequency of the incoming RF signal at its antenna, signals from other simultaneous transmissions can also be rectified and potentially interfere with the down-converted data signal. However, MIXIQ is highly robust to such interference caused by other WiFi transmitters. This is because the transmit power of the interfering devices is not concentrated on the three data subcarriers, but rather distributed among the 24 subcarriers and two pilot tones (in case of the smallest size RU that has 26 subcarriers, while for larger RUs, the power is even further distributed). Hence, the interference power at the three target data subcarriers becomes much lower.

Even if the interference on the down-converted data subcarriers exceeds the threshold that can be tolerated by MIXIQ's QAM-64 demodulator, the data can be protected by compromising on the bit rate and adapting it based on the interference. This is accomplished by selecting a *subset* (instead of all) of the QAM-64 constellation points as the alphabet, thereby increasing the minimum distance between any two constellation points. This in turn increases $\frac{E_s}{N_0+I}$ to more than 25dB, where I is the power of the interference on the data subcarriers. Our evaluations in Section 8.4 reveal MIXIQ's higher degree of robustness to varying levels of interference.

6 SYSTEM CONFIGURATION

We now describe how MIXIQ is able to co-exist with a standard 802.11ax WiFi network by only occupying 10% of a single channel bandwidth (22 MHz during operation).

802.11ax uplink trigger mode: In 802.11ax, there is a multi-user mode of operation defined for uplink OFDMA (i.e. from the clients to the AP), which allows a single WiFi channel to be split among several clients. Therefore, clients can concurrently send their data in a particular portion of the channel, called resource unit(s) (RU) allocated to them. MIXIQ configures the uplink of the network to work in trigger mode and its transmitter is chosen to be one of the clients, which is assigned a RU that has the smallest size possible, i.e. consisting of 26 sub-carriers (24 data and two pilot tones), each 78.125 KHz wide, making the whole RU to be 2.2MHz.

Packet structure: MIXIQ adapts the encoding and the decoding of data to 802.11ax's structure of the packet payload. The packet's payload consists of blocks of data bits, each followed by a set of parity bits. Note that we can only control the data bits, while the parity bits are automatically determined by the LDPC encoding matrix based on the data bits. Hence, MIXIQ embeds the data + helper (LO) signals in the OFDM symbols that correspond to the data bits and simply bypass the symbols that correspond to the parity bits. We set the LDPC code rate to 5/6, which is the highest code rate in 802.11ax for QAM-64, to minimize the throughput loss due to the inactivity during the parity bits.

Preamble insertion: MIXIQ uses the first two symbols in the data payload to create a custom preamble. MIXIQ modulates each of the three subcarriers (that is used for data) with constellation point C_1 = 1+j (has the most distance from the origin in QAM-64) in the first symbol time and $C_2 = -C_1$ in the second symbol time. MIXIQ's receiver uses this preamble for (1) detecting the beginning of a packet, (2) finding the reference amplitude and phase values to perform IQ demodulation successfully, and (3) doing distortion control as described in §5.1.2.

Cyclic prefix: In 802.11ax, like other OFDM WiFi signals, the 12.8μs OFDM symbol interval is followed by a guard interval, called cyclic prefix with a specific length that can be as short as 3.2μs. This cyclic prefix is exactly taken from the beginning of the OFDM symbol. MIXIQ's receiver does not use this cyclic prefix for demodulation and the 12.8μs symbol is directly correlated with the Cosine and Sine waveforms. Hence, we set the length of the cyclic prefix to its minimum of 3.2μs to minimize the throughput loss from cyclic prefix overhead. In this case, 3 (number of subcarriers) $\times$ 8 (number of bits per QAM-64 symbol) = 24 bits are sent per 16μs (OFDM symbol time + cyclic prefix).

Pilot tone phase variation: Even though the amplitude of the pilot tones remains constant within the entire packet, their phases take different values, from $\{0,\pi\}$ per symbol according to the pattern defined by the standard. As a result, the phase of the QAM-64 symbols on the down-converted data subcarriers have π offset from the true value at some of the symbol times. But since the pattern is known, the receiver can simply reverse the phase at these symbol times to compensate for the phase offset.

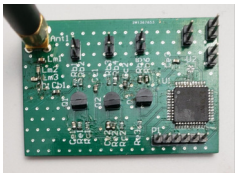

(a) MIXIQ Prototype.

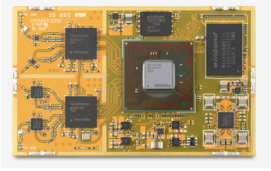

(b) IPQ6010 module.

Figure 6: MIXIQ 's TX and RX hardware.

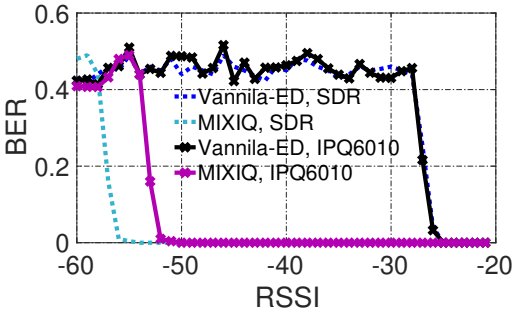

Figure 7: Sensitivity of MIXIQ vs. Vanilla-ED.

7 IMPLEMENTATION

7.1 Tag hardware

Figure 6(a) shows a PCB prototype of our MIXIQ's receiver. The components employed are as follows.

Antenna + rectifier: A W24-SSMA-M 2.4GHz small whip antenna with 2dBi gain. Also, Infineon BAT63-02V RF Schottky diode [12] serves as the RF rectifier with a π matching network between it and the antenna, resulting in the conversion ratio plotted in Figure 3.

High-impedance sub-MHz Amplifiers and ADC buffers: ON-Semi 2N3904 general-purpose bipolar transistors [22] are used to implement the two-stage common-emitter amplifier(§5.1) as well as the common-collector impedance buffer between the amplifier and ADC (§5.2).

ADC: Texas Instruments ADS7042 serves as the ADC. It draws 122.9μA from a 1.5v DC power supply during analog-to-digital conversion at 1MSPS with a 12-bit resolution.

Baseband logic: A Xilinx XC2C64A-7VQGC CoolRunnerII CPLD [50], which is compatible with a 1.5v logic level is used to implement the tasks of digital IQ demodulation, preamble detection, and pilot tone phase adaptation. Even though this CPLD is highly optimized for power efficiency, it provides enough resources to do all the arithmetic required for these tasks. In addition, MIXIQ is able to store the values of sine and cosine waveforms required for IQ demodulation in the memory blocks of the CPLD. In total, 43 of the total 64 macro-cells (67%) of XC2C64 are used to implement the full functionality of the digital parts of the receiver.

ADC and logic clock oscillator: Two SiTime SiT1576 [34] (a micro-power MEMS oscillator) are used to produce the 1MHz ADC clock and the 2MHz CPLD clock.

CMOS Simulation: We also conduct a CMOS simulation of the analog/digital pipeline after the rectifier using Cadence Virtuoso IC Design software. This allows us to test the functionality and estimate the power consumption of MIXIQ's building blocks in TSMC 130nm technology. For the ADC, we employ the design proposed in [43] which is a 10-bit charge-redistribution analog-to-digital converter consuming only 1.9μA from a 1V DC voltage source. Hence, we set the overall gain of the amplifier+buffer stages to 63dB (6dB higher than the gain of the BJT amplifiers) to appropriately compensate for the lower resolution of the ADC compared with the off-the-shelf one used in our prototype (ADS7042).

7.2 802.11ax TX

We implement MIXIQ on both a commercially-available WiFi 6 chipset (the IPQ6010 [27]) as well as in MATLAB's WLAN 802.11ax PHY-MAC stack. The MATLAB emulation allows us to evaluate the effect of hardware imperfections and to ensure that the results can generalize to any 802.11ax implementation.

Our implementation is based on a version of openWRT (an open-source, linux-based driver that supports a myriad of commercial Wireless routers) developed for 8-devices Mango-I [42] (Figure 6(b)) which is an IPQ6010 daughterboard that is connected to Mango DVK board [41]. This version of openWRT provides APIs for configuring IPQ6010 to operate as a client in the uplink trigger mode while using one 26-tone resource unit to send its packet to the AP with QAM-64 and $\frac{5}{6}$-rate LDPC as modulation and coding schemes, respectively. We choose the first RU of the first 802.11ax WiFi channel (i.e. the RU that starts at 2402.59MHz and end at 2404.61MHz).

In addition, the 8-devices openWRT allows us to send raw payloads over 802.11ax WiFi packets, i.e. no protocol such a IPV4 and TCP on top of it. That allows us to send our reverse engineered payloads that result in the data+helper structure that we discuss in §4.2. Throughout our experiments, we configure the transmit power of the Mango-I board to 17dBm, to mimic a cellphone device.

Our emulation uses MATLAB's WLAN toolbox (for 802.11ax PHY-MAC stack) for embedding the data+helper signal within the payload of 802.11ax packets. It allows us to do the required reverse engineering on the payload of the packet such that the desired sub-carriers {-13,-12,-11} are made to contain data while the rest of the sub-carriers are nullified by assigning lowest constellation points to them. In addition, later during the evaluation of an audio application in §8.5, we use MATLAB to encode 128 Kbps audio streams to data bits that are used to modulate MIXIQ's data transmission.

8 EVALUATION

We characterize MIXIQ 's overall performance, followed by a validation of the benefits of its key design components. We then present a case study of MIXIQ 's potential through a hearable application that we prototyped.

8.1 MIXIQ's Overall Performance

MIXIQ Sensitivity: Figure 7 compares the bit error rate (BER) of MIXIQ against Vanilla-ED (§2). The Vanilla-ED is implemented with the same RF rectifier, BAT63-02, and Texas Instruments TLV7011 micro-power comparator [38]). We also plot the measurement results with MATLAB+SDR to show that we achieve the similar gains regardless of what WiFi device we use as TX.

Metric	MIXIQ	Vanilla-ED
Throughput (Kbps)	1125	125
Spectral Eff. (bps/Hz)	0.51	0.0057

Table 1: MIXIQ vs. Vanilla-ED

Component	PCB prototype	CMOS simulation
Amplifiers	132.9μW	29.6μW
ADC	184.3μW	1.9μW
IQ demodulator	47.4μW	9.3μW
Total	**364.6μW**	**40.8μW**

Table 2: MIXIQ's power consumption: (PCB vs. CMOS simulation).

In order to measure the MIXIQ 's BER, we modulate a total of 100,000 random bits on its three data subcarriers {-13,-12,-11} and compare the output of its IQ demodulator with the original bits to calculate BER, and repeat this for various RSSI of the 802.11ax WiFi packet, ranging from -60dBm to -20dBm. To vary RSSI, we connect the RF ports of the TX device (SDR or WiFi) to the receiver (Vanilla-ED or MIXIQ) via a coaxial cable, in series with a Renesas Electronics F1950 digitally-controlled variable attenuation module [28]. Also, up to two Mini-Circuits fixed 30dB attenuators [19] are added to the chain for covering lowest RSSI values. Similarly, for obtaining the BER of the Vanilla-ED, we modulate 100,0000 bits on 802.11ax symbols according to the OOK method proposed in [13] (even though the method in [13] is for 802.11ac, the same technique for emulating OOK using OFDM symbols is applicable to 802.11ax as well). It can be seen that to achieve near zero (<0.0001) BER, Vanilla-ED needs an RSS > -26dBm, whereas MIXIQ can work at RSS as low as -52dBm. In other words, *MIXIQ improves the receive sensitivity by > 25 dB over that of Vanilla-ED.*

We also see that the 802.11ax emulation with MATLAB and SDR and experimental results on IPQ6010 are very similar which shows that our results should generalize to any 802.11ax implementation. The performance of the Vanilla-ED is identical in emulation and experimentation. The performance of the MIXIQ receiver in emulation and experimentation are only 3dB apart (possibly due to small hardware imperfections which introduce additional interfering terms to the data+helper signal).

MIXIQ Spectral Efficiency: Table 1 shows MIXIQ 's performance in terms of throughput and spectral efficiency and compares these against the Vanilla-ED's performance. *MIXIQ not only has 9× better throughput; it also occupies 10× less bandwidth than the Vanilla-ED (2.2MHz compared to 22MHz).* As a result, MIXIQ 's spectral efficiency is significantly better (89×) than that of the Vanilla-ED. The throughput increase from Kbps to Mbps also offers a substantial spectral efficiency gain of 9×, even if the rest of the 22MHz channel is not utilized by any other WiFi devices to avoid interference.

Range: Figure 8(a) shows the experimental setup for our range experiment. It consists of a standard WiFi 6 TX device (Mango-I IPQ6010 evaluation board) and MIXIQ PCB tag being in the Line of Sight (LoS) of each other. At one end of this LoS link, the WiFi TX devices transmits the reverse engineered *data+helper* packets at 17dBm via a 5dBi 2.4GHz whip antenna. At the other end of the link, the tag demodulates the data bits within the packets at d meters away from the WiFi TX device.

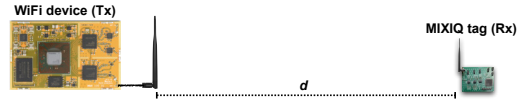

(a) Experimental Setup.

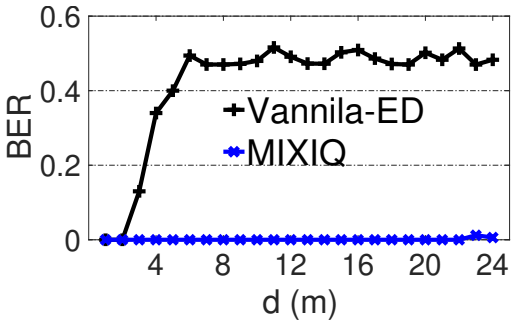

(b) BER vs distance.

Figure 8: MIXIQ 's range vs. Vanilla-ED.

To determine the range, i.e. the maximum distance at which the tag is able to decode data with extremely low BER, we locate the tag at different distances , d, from the WiFi TX device in 1 meter steps. The nodes were placed in a long 24 meter hallway. At each location, we measure the BER the same way as we did in the Sensitivity experiment. Note that the same setup and measurement procedure can be done for the Vanilla-ED receiver, too.

Figure 8(b) shows the experimental results. We see that in the LoS scenario, Vanilla-ED can successfully decode at only 2–3 meters away from the WiFi TX device whereas MIXIQ is able to decode the data bits with zero or near-zero BER across all the distances (1–24 meters). Thus, Figure 8(b) shows that MIXIQ has at least 10× higher range than Vanilla-ED although this may be even larger since MIXIQ 's BER is still low at the end of the hallway.

8.2 MIXIQ Power Benchmarks

Table 2 shows the breakdown of power consumption of MIXIQ 's PCB prototype and also provides, as reference, simulation numbers if such a system were to be implemented with CMOS.

While the values in Table 2 shows power consumption when the receiver is in data modulation mode without performing any other task, we note that the CPLD used in the digital demodulator design has enough resources remaining for also doing gain control, power management, and other tasks. Unlike data reception, these other tasks do not happen very frequently and also require only a few μA from the power supply of the CPLD. Therefore, their overall contribution to the average power consumption is negligible.

We see that the overall consumption of our PCB-based implementation is 364.6μW and the power consumed by the CMOS simulated version is 40.8μW. The achievable bitrate is 1.125Mbps which translates to 3248 bits/μJ and 27,573 bits/μJ for MIXIQ 's PCB prototype and CMOS simulation, respectively.

Work	WiFi standard	Modulation	Sensitivity (dBm)	Spectral Eff. (bps/kHz)	Energy Eff. (bits/μJ)	PCB prototype
[10] (2017)	802.11a (5.8GHz)	FSK	-67, -70	11, 1.4	746, 93	No
[1] (2018)	802.11g/n (2.4GHz)	OOK	-72	2.8	659	No
[11] (2019)	802.11ba (5.8GHz)	OOK	-83	2.8	285	No
[48] (2020)	802.11b (2.4GHz)	OOK	-42.5	0.3	2286	No
MIXIQ (2021)	802.11ax (2.4GHz)	64-QAM	-52	51	3248(PCB), 27573 (CMOS simulation)	Yes

Table 3: Comparison of MIXIQ against state-of-the-art IC-based Envelope Detector designs.

For the CMOS simulation, the power consumption of all blocks reduces with respect to their PCB counterparts; but the most significant reduction happens to the ADC; ADC's power consumption reduces by 100× compared to the discrete part mounted on the PCB. This results from an ADC power optimization technique called *charge distribution* that we borrow from recent work on ultra low power ADC [43] which allows us to design a high-resolution yet ultra low power ADC.

Thus, we see that MIXIQ provides much improved performance while sacrificing a small amount of energy efficiency in the process.

8.2.1 How does MIXIQ compare to enhanced IC-based envelope detector designs? Table 3 lists the performance of prominent state-of-art enhanced ED IC designs that can directly receive data from standard WiFi devices. As expected, these designs mostly outperform MIXIQ in terms of receive sensitivity — they achieve better than -70dBm sensitivity while MIXIQ provides -52dBm (the -52dBm sensitivity is still a > 25dB improvement of a PCB prototyped Vanilla-ED). However, our proposed design has two important benefits over other efforts. First, it boosts spectral efficiency by 5× – 50× compared to other designs which can result in better bandwidth usage. Second, as we have described, our design can be easily prototyped using off-the-shelf components. Thus, MIXIQ bridges the gaps between uplink and downlink performance of an easy-to-prototype backscaatter tag.

8.3 Impact of MIXIQ's Design Choices

Now, we validate the effect of MIXIQ's design choices and their contribution to its overall performance.

Comparison between 0,1,2 - stage amplifiers. Figure 9 compares the sensitivity for different modulation schemes (and consequently different bitrates) when we choose different amplifier pipelines. The result is obtained by repeating the sensitivity experiment of Section 8.1. for 0, 1, and 2 amplifiers and WiFi TX. We see two interesting observations. First, using a two-stage amplifier (as in MIXIQ) significantly improves the sensitivity and thus we can achieve a sensitivity of -52dBm for 64-QAM. Second, there is not a significant sensitivity difference between 1-stage and 2-stage for low order modulations, especially BPSK. The reason is that when the RSS < -55dBm, the passive rectifier is operating close to its physical limits and stops converting the signal; hence, irrespective of the amount of amplification (1 or 2 stages), we are unable to improve sensitivity to below -55dBm. Consequently, *the sensitivity for different modulations are approximately the same when using a two-stage amplifier.*

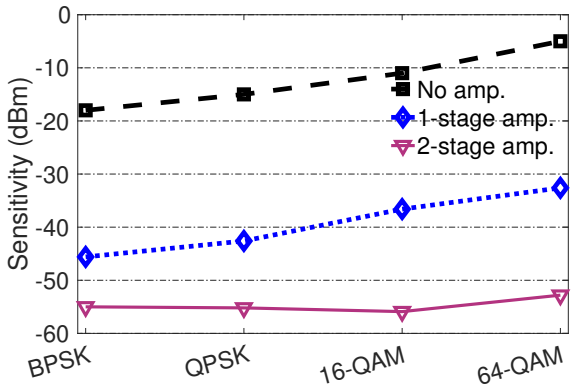

Figure 9: Sensitivity of different amplifier pipelines.

Effect of number of subcarriers Figure 10 shows the energy efficiency (bit/μJ) versus the number of subcarriers when we use the same architecture of MIXIQ but at different sampling rates to demodulate the sub-carriers. *We see that three sub-carriers results in the highest efficiency of around 3000 bits/μJ*; performance rapidly degrades thereafter due to the higher sampling rates needed to perform IQ demodulation. Note that the power consumption of the amplifier remains the same as we are still in sub-MHz regime and leverage the benefits of the μW amplifiers (§5.1). Hence, the sensitivity remains the same across the number of subcarriers in Figure 10.

Rationale for choice of subcarriers. To understand which data sub-carriers provide best performance, we look at the extent of inter-modulation and residual terms that exist at different data sub-carriers, Figure 11. We generate random data bits at the sub-carriers and measure the signal to inter-modulation interference ratio (SIR, Fig. 11(a)) and signal to residual terms ratio (SRR, Fig. 11(b)) at the output of MIXIQ 's demodulator. This experiment is done by placing the WiFi Tx and MIXIQ antennas 1 meters away from each other, and with the WiFi TX device transmitting WiFi packets at 17dBm. It can be observed that for subcarriers -13,-12,-11 both SIR and SRR are sufficiently above 25dB allowing for 64-QAM modulations. Subcarrier -10 has a very good SIR as it is far from the inter-modulation terms; however, it suffers from residual terms are still large and therefore the overall ratio between the signal and the unwanted terms is <25dB. Thus, *the three sub-carriers -13, -12, and -11 offer good robustness against both inter-modulation and residual impacts and form the rationale behind MIXIQ 's choice of data sub-carriers.* For brevity, we do not include results for different

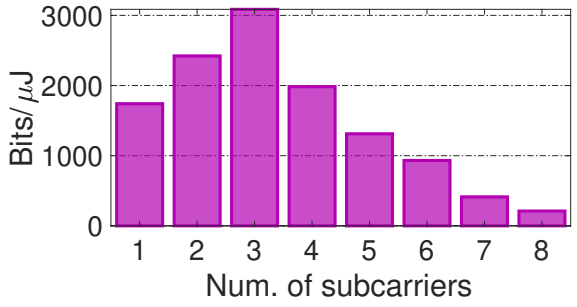

Figure 10: Bits/μJ vs. number of subcarriers.

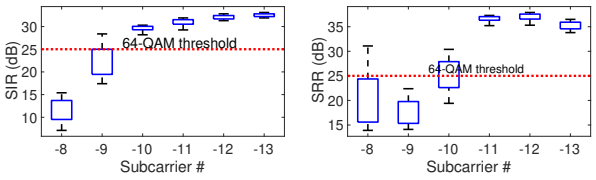

(a) SIR (b) SRR

Figure 11: SIR and SRR across data subcarriers.

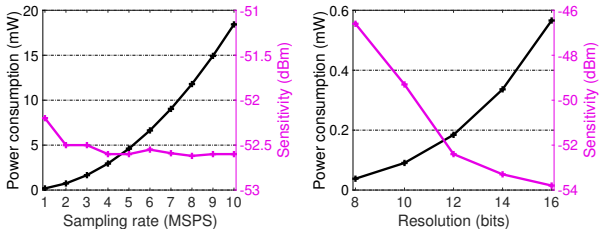

(a) Sampling rate (b) Resolution

Figure 12: Sensitivity/power vs. ADC specs.

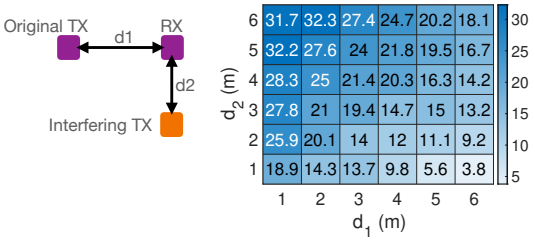

Figure 13: SINR at different locations.

distances between TX and RX. MIXIQ shows the same behavior across different distances except when the tag is very close (<20cm) to the TX device in which case non-linear distortions at the output of the rectifier overwhelm the modulator.

Effect of ADC sampling rate and resolution: Figure 12 captures ADC's performance and sensitivity as a function of its resolution and sampling rate. Increasing the sampling rate as well as the resolution of the ADC, boosts decoding sensitivity, but is also accompanied by a rapid increase in power consumption and whereas slight improvement in sensitivity. *MIXIQ strikes a balance between the sensitivity and power consumption to operate the ADC at 12-bit resolution and 1 MSPS.*

8.4 Co-existence with other WiFi devices

We now capture MIXIQ's robustness to other WiFi clients that transmit in other resource units of the 802.11ax WiFi channel in parallel. Figure 13 shows our experimental setup. We used two IPQ6010-based devices, one as MIXIQ's (original) TX and one as the interfering TX (another WiFi client), at distances d_1 and d_2 from MIXIQ's RX, respectively. We conducted this experiment in a 6m×6m space in our hardware lab. The original TX transmits based on MIXIQ's signaling (wherein only three data sub-carriers are used and the rest are null), while the interfering TX transmits over the entire resource unit it is using, both with the same transmit power of 17dBm. Now, at different d_1 and d_2, we capture the output of the digital IQ demodulator at the three data subcarriers and calculate the minimum SINR among these three subcarriers. Figure 13 shows the heat-map of the SINR for different distances. It is observed that when the interfering TX is 3m or more away from RX, the SINR is >25dB (original TX is 3m or closer to RX), thereby allowing for 64-QAM demodulation; while lower order modulations such as 16-QAM should be possible at farther distances. *MIXIQ's potential for co-existence, opens the door for improved (aggregate) network throughputs in the future.*

8.5 Ultra-low Power Audio Streaming

An enhanced ultra-low power receiver can benefit any IoT or wearable application where downlink overhead is non-trivial. We evaluate the use of MIXIQ in one such application, audio streaming to a Hearable device like an earphone.

We show the benefits of a better receiver using a novel WiFi-based VoIP or audio streaming prototype that uses MIXIQ achieve better performance. We consider a WiFi TX device (IPQ6010 evaluation board) that is transmitting the VoIP signal (or a music stream) with an audio quality of 128 Kbps at 17dBm. Our goal is to investigate the quality of the audio received with MIXIQ's receiver and compare it with that of Vanilla-ED.

Digital audio player (DAP): Figure 14 shows the design of our low power digital audio player (connected via a 3.5mm jack connector to the radio) that mimics a simple version of a hearable. While the audio front-end is not our innovation, a full system prototype allows us to holistically evaluate performance. It consists of a TPL0501-100DCNR[39] ultra low power digital potentiometer for converting the received 8-bit audio samples to analog values. The logic resources of the CPLD of the receiver are also used to communicate with the digital potentiometer through SPI protocol. Since the analog output of the potentiometer varies between 0 and V_p (Figure 14), the magnitude of the signal and hence the volume of the voice being played depends on how big V_p is. To isolate the high impedance of the digital potentiometer (100kΩ) and the low impedance of speaker (64 Ω), we use a unity gain stage consisting of a LPV511MG[37] ultra low power op-amp.

Performance: Figure 15 shows the results when the WiFi TX (IPQ6010 evaluation baord) transmits bits of audio on top of 802.11ax according to MIXIQ's signaling (data+helper) with an 17dBm transmit power. The WiFi TX device is at different distances from the wireless earphone (i.e. our DAP) worn by a person who is doing body movements according to a known pattern for 5 minutes at each point of the hallway next to the lab where the receiver is

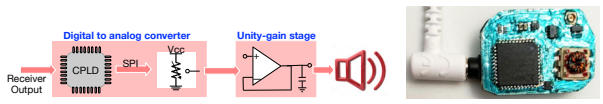

(a) Block diagram (b) Prototype

Figure 14: Ultra low power digital audio player.

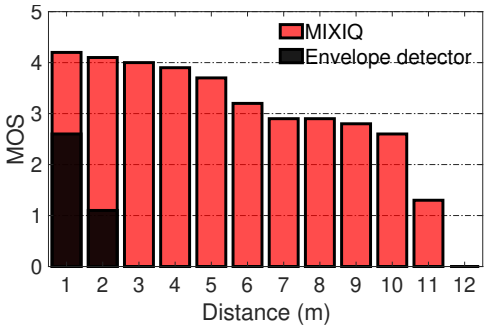

Figure 15: MOS vs. distance.

placed (same experimental setup as §8.1), except that the tag is worn by a person rather than being static in the Line of Sight).

We see that MIXIQ has good MOS scores (> 3) when the IPQ6010 evaluation board is < 7m since signal strength of the data is fairly good, but slightly degrades to a little below 3 MOS scores when the IPQ6010 evaluation board is 6–10 meters. Finally, the quality drops quite a bit at 10-11 meters until MOS can no longer be measured at 12m, as there is a lot of noise in the audio. On the other hand, the Vanilla-ED fails to deliver good quality audio even at 1 meter and MOS cannot be measured even at >2m, when it delivers just noise. *This 10× increase in operational range can be attributed to MIXIQ 's improved sensitivity even at higher data rates.* Note that the results of this experiment show lower operational range than the range experiment done in §8.1 despite having the same experimental setup. This is due to human body effects that introduce additional signal loss and thus limit the range.

9 RELATED WORK

Ultra low power receivers: There has been considerable work on improving the performance of envelope detectors and ultra low power receivers. An important category is wake-up radios with boosted sensitivity (better than -70 dBm) at ultra low power consumption (<100 μW). The focus of wake up radios is primarily on sensitivity and low power and not spectral efficiency. Hence they are typically designed for very low bit rates (a few kbps or less), which makes them suitable primarily for wake-up applications [9, 21, 29, 31, 47]. However, newer efforts in the field of RF IC design achieve up to tens of Kbps at a higher sensitivity of -70dBm to -97dBm. While some of these designs need specialized transmitter and carriers [23, 26, 31, 32], there are also several recent ultra low power radio designs that can directly receive OOK, FSK, or QPSK signals emulated on standard WiFi packets [1, 10, 11, 48], which makes them compliant with commodity WiFi networks while achieving up to -80dBm and 62.5kbps bitrate at μW regime.

Backscatter research: There has been a large volume of work focused on frequency-shifted backscatter with commodity devices. Among these, some use analog elements like tunnel diodes [2, 44] and impedance transformers [30] to generate and/or amplify the backscattered signal. Our work is significantly different in that we leverage such analog elements in the receiver design rather than in the transmitter.

The use of a helper signal for backscatter transmission is quite common (and referred to as bi-static backscatter). These are often used to enable a backscatter transmitter to talk to a commodity radio such as WiFi AP or Bluetooth radio [13, 14, 24, 35, 46, 51, 53–57]. Their focus is on the transmitter whereas we bring to bear the ideas in the context of an ultra-low power receiver that can receive from a commodity WiFi radio.

External-helper tone receivers: Our work is related to recent receiver designs that use an external helper tone to convert envelope detectors to mixers [7, 25]. However, these works focus primarily on enabling IQ detection, without improving sensitivity, spectral efficiency, or power consumption. In addition, these methods require a separate device to generate the external helper tone whereas we can leverage 802.11ax to achieve this goal. MIXIQ provides a complete design that significantly improves all aspects of the energy-performance tradeoff, while working with commodity WiFi devices. The most similar work to ours is [18] which also uses the external helper idea to enable communication with standard WiFi devices. However, it uses a separate "interferer" device at 550MHz which provides the helper tone signal whereas we do not require a separate helper device.

10 CONCLUSIONS

In this paper, we tackle the long-standing problem of designing better ultra low power receivers. We present a new architecture, MIXIQ , that builds on the idea of an external oscillator-based mixer and synergistically complements it with a novel hybrid baseband pipeline. That enables dramatic improvements in both sensitivity and spectral efficiency, while operating in the μW power regime. MIXIQ is compatible with WiFi radios via a novel signaling method that leverages OFDMA for generating the external oscillator signal. Our results show that very interesting on-body applications can be made possible by having an ultra low power radio that can deliver a superior energy-efficient downlink performance.

Our work can be improved in a number of ways that we are continuing to explore. MIXIQ 's bit rate is currently limited to 1.1Mbps, which can be low in scenarios where multiple nodes want to receive high-rate data simultaneously without occupying the WiFi network traffic too much. Our current design is also limited in its ability to work in the presence of multiple concurrent WiFi devices which will interfere with the downlink transmissions. Finally, we show that we can support a limited level of concurrency (three nodes) but this can be improved to support more tags. In future work, we are looking at new signaling and multiplexing techniques that can build on MIXIQ to tackle these problems.

ACKNOWLEDGMENTS

We thank the anonymous reviewers and shepherd of our paper for their detailed comments and guidance in preparing the final draft. This research was partially supported by NSF grant 1815347.

REFERENCES

[1] E. Alpman, A. Khairi, R. Dorrance, M. Park, V. S. Somayazulu, J. R. Foerster, A. Ravi, J. Paramesh, and S. Pellerano. 802.11g/n compliant fully integrated wake-up receiver with -72 dbm sensitivity in 14 nm finfet cmos. *IEEE Journal of Solid-State Circuits*, 53(5):1411–1422, 2018.

[2] F. Amato, C. W. Peterson, B. P. Degnan, and G. D. Durgin. Tunneling rfid tags for long-range and low-power microwave applications. *IEEE Journal of Radio Frequency Identification*, 2(2):93–103, 2018.

[3] Avago. *HSMS-285x Series, Surface Mount Zero Bias Schottky Detector Diodes.*

[4] J. E. Bardram. The cams esense framework: Enabling earable computing for mhealth apps and digital phenotyping. In *Proceedings of the 1st International Workshop on Earable Computing*, EarComp'19, page 3–7, New York, NY, USA, 2019. Association for Computing Machinery.

[5] D. Bharadia, K. R. Joshi, M. Kotaru, and S. Katti. Backfi: High throughput wifi backscatter. *ACM SIGCOMM Computer Communication Review*, 45(4):283–296, 2015.

[6] R. R. Choudhury. Earable computing: A new area to think about. In *Proceedings of the 22nd International Workshop on Mobile Computing Systems and Applications*, HotMobile '21, page 147–153, New York, NY, USA, 2021. Association for Computing Machinery.

[7] J. F. Ensworth, A. T. Hoang, and M. S. Reynolds. A low power 2.4 ghz superheterodyne receiver architecture with external lo for wirelessly powered backscatter tags and sensors. In *2017 IEEE International Conference on RFID (RFID)*, pages 149–154, May 2017.

[8] G. Haas, E. Stemasov, M. Rietzler, and E. Rukzio. *Interactive Auditory Mediated Reality: Towards User-Defined Personal Soundscapes*, page 2035–2050. Association for Computing Machinery, New York, NY, USA, 2020.

[9] X. Huang, S. Rampu, X. Wang, G. Dolmans, and H. de Groot. A 2.4ghz/915mhz 51μw wake up receiver with offset and noise suppression. In *2010 IEEE International Solid-State Circuits Conference - (ISSCC)*, pages 222–223, Feb 2010.

[10] J. Im, H. Kim, and D. D. Wentzloff. A 335μw -72dbm receiver for fsk back-channel embedded in 5.8ghz wi-fi ofdm packets. In *2017 IEEE Radio Frequency Integrated Circuits Symposium (RFIC)*, pages 176–179, 2017.

[11] J. Im, H. Kim, and D. D. Wentzloff. A 220 μw -83 dbm 5.8 ghz third-harmonic passive mixer-first lp-wur for ieee 802.11ba. *IEEE Transactions on Microwave Theory and Techniques*, 67(7):2537–2545, 2019.

[12] Infineon. *BAT6302-V Silicon Schottky Diode.*

[13] V. Iyer, V. Talla, B. Kellogg, S. Gollakota, and J. Smith. Inter-technology backscatter: Towards internet connectivity for implanted devices. In *Proceedings of the 2016 conference on ACM SIGCOMM 2016 Conference*, pages 356–369. ACM, 2016.

[14] B. Kellogg, V. Talla, S. Gollakota, and J. R. Smith. Passive wi-fi: Bringing low power to wi-fi transmissions. In *NSDI*, volume 16, pages 151–164, 2016.

[15] E. Khorov, A. Kiryanov, A. Lyakhov, and G. Bianchi. A tutorial on ieee 802.11ax high efficiency wlans. *IEEE Communications Surveys Tutorials*, pages 1–1, 2018.

[16] Y. Li, Z. Chi, X. Liu, and T. Zhu. Passive-zigbee: Enabling zigbee communication in iot networks with 1000x+ less power consumption. In *Proceedings of the 16th ACM Conference on Embedded Networked Sensor Systems*, SenSys '18, page 159–171, New York, NY, USA, 2018. Association for Computing Machinery.

[17] Y. Ma, X. Hui, and E. C. Kan. 3d real-time indoor localization via broadband nonlinear backscatter in passive devices with centimeter precision. In *Proceedings of the 22Nd Annual International Conference on Mobile Computing and Networking*, MobiCom '16, pages 216–229, New York, NY, USA, 2016. ACM.

[18] V. Mangal and P. R. Kinget. A wake-up receiver with a multi-stage self-mixer and with enhanced sensitivity when using an interferer as local oscillator. *IEEE Journal of Solid-State Circuits*, 54(3):808–820, 2019.

[19] Mini-Circuits. *30 dB Fixed Attenuator, DC - 6000 MHz, 50Ω.*

[20] S. Naderiparizi, Z. Kapetanovic, and J. R. Smith. Rf-powered, backscatter-based cameras. In *2017 11th European Conference on Antennas and Propagation (EUCAP)*, pages 346–349, 2017.

[21] S. Oh, N. E. Roberts, and D. D. Wentzloff. A 116nw multi-band wake-up receiver with 31-bit correlator and interference rejection. In *Proceedings of the IEEE 2013 Custom Integrated Circuits Conference*, pages 1–4, Sep. 2013.

[22] On Semiconductor. *General Purpose Transistors.*

[23] J. N. Pandey, J. Shi, and B. P. Otis. A 120μw mics/ism-band fsk receiver with a 44μw low-power mode based on injection-locking and 9x frequency multiplication. *2011 IEEE International Solid-State Circuits Conference*, pages 460–462, 2011.

[24] Y. Peng, L. Shangguan, Y. Hu, Y. Qian, X. Lin, X. Chen, D. Fang, and K. Jamieson. Plora: A passive long-range data network from ambient lora transmissions. In *Proceedings of the 2018 Conference of the ACM Special Interest Group on Data Communication*, SIGCOMM '18, pages 147–160, New York, NY, USA, 2018. ACM.

[25] C. Pérez-Penichet, C. Noda, A. Varshney, and T. Voigt. Battery-free 802.15.4 receiver. In *Proceedings of the 17th ACM/IEEE International Conference on Information Processing in Sensor Networks*, IPSN '18, pages 164–175, Piscataway, NJ, USA, 2018. IEEE Press.

[26] N. Pletcher, S. Gambini, and J. Rabaey. A 52 μw wake-up receiver with-72 dbm sensitivity using an uncertain-if architecture. *Solid-State Circuits, IEEE Journal of*, 44:269 – 280, 02 2009.

[27] Qualcomm. *Qualcomm Networking Pro 400 Platform.*

[28] Renesas Electronics America Inc. *7-bit 0.25 dB Digital Step Attenuator 150MHz to 5000MHz.*

[29] N. E. Roberts, K. Craig, A. Shrivastava, S. N. Wooters, Y. Shakhsheer, B. H. Calhoun, and D. D. Wentzloff. A 236 nw -56.5 dbm sensitivity bluetooth low-energy wake up receiver with energy harvesting in 65 nm cmos. 2017.

[30] M. Rostami, K. Sundaresan, E. Chai, S. Rangarajan, and D. Ganesan. Redefining passive in backscattering with commodity devices. In *The 26th Annual International Conference on Mobile Computing and Networking*, 2020.

[31] C. Salazar, A. Cathelin, A. Kaiser, and J. Rabaey. A 2.4 ghz interferer-resilient wake-up receiver using a dual-if multi-stage n-path architecture. *IEEE Journal of Solid-State Circuits*, 51(9):2091–2105, Sep. 2016.

[32] N. Saputra and J. R. Long. A fully integrated wideband fm transceiver for low data rate autonomous systems. *IEEE Journal of Solid-State Circuits*, 50(5):1165–1175, 2015.

[33] T. S. P. See, C. W. Kim, T. M. Chiam, Y. Ge, A. A. P. Wai, and Z. N. Chen. Study of dynamic on-body link reliability for wban systems. In *2012 IEEE Asia-Pacific Conference on Antennas and Propagation*, pages 112–113, 2012.

[34] SiTime. *1.2mm^2 μPower, Low-Jitter, 1Hz – 2.5 MHz Super-TCXO*, Mar. 2018. Rev. 1.3.

[35] V. Talla, M. Hessar, B. Kellogg, A. Najafi, J. R. Smith, and S. Gollakota. Lora backscatter: Enabling the vision of ubiquitous connectivity. *arXiv preprint arXiv:1705.05953*, 2017.

[36] V. Talla and J. R. Smith. Hybrid analog-digital backscatter: A new approach for battery-free sensing. In *2013 IEEE International Conference on RFID (RFID)*, pages 74–81, 2013.

[37] Texas Instruments. *LPV511 Micropower, Rail-to-Rail Input and Output Operational Amplifier.* Rev. D.

[38] Texas Instruments. *Small-Size, Micro-Power, Low-Voltage Comparators.* Rev.C.

[39] Texas Instruments. *TPL0501 256-Taps, Single-Channel, Digital Potentiometer With SPI Interface.* Rev. C.

[40] Texas Instruments. *Ultra-Low Power, Ultra-Small Size, 12-Bit, 1-MSPS, SAR ADC.* Rev. A.

[41] https://shop.8devices.com/MANGO-DVK. Mango DVK.

[42] https://shop.8devices.com/MANGO-I. Mango-I Wi-Fi 6 module.

[43] M. van Elzakker, E. van Tuijl, P. Geraedts, D. Schinkel, E. Klumperink, and B. Nauta. A 1.9μw 4.4fj/conversion-step 10b 1ms/s charge-redistribution adc. In *2008 IEEE International Solid-State Circuits Conference - Digest of Technical Papers*, pages 244–610, 2008.

[44] A. Varshney, A. Soleiman, and T. Voigt. Tunnelscatter: Low power communication for sensor tags using tunnel diodes. In *The 25th Annual International Conference on Mobile Computing and Networking*, pages 1–17, 2019.

[45] D. Vasisht, G. Zhang, O. Abari, H.-M. Lu, J. Flanz, and D. Katabi. In-body backscatter communication and localization. In *Proceedings of the 2018 Conference of the ACM Special Interest Group on Data Communication*, SIGCOMM '18, pages 132–146, New York, NY, USA, 2018. ACM.

[46] A. Wang, V. Iyer, V. Talla, J. R. Smith, and S. Gollakota. Fm backscatter: Enabling connected cities and smart fabrics. In *NSDI*, pages 243–258, 2017.

[47] P. P. Wang, H. Jiang, L. Gao, P. Sen, Y. Kim, G. M. Rebeiz, P. P. Mercier, and D. A. Hall. A near zero power wake up receiver achieving -69 dbm sensitivity. *IEEE Journal of Solid-State Circuits*, 53(6):1640–1652, June 2018.

[48] P. P. Wang, C. Zhang, H. Yang, D. Bharadia, and P. P. Mercier. 20.1 a 28µw iot tag that can communicate with commodity wifi transceivers via a single-side-band qpsk backscatter communication technique. In *2020 IEEE International Solid-State Circuits Conference - (ISSCC)*, pages 312–314, 2020.

[49] H. Watanabe and T. Terada. Manipulatable auditory perception in wearable computing. In *Proceedings of the Augmented Humans International Conference*, AHs '20, New York, NY, USA, 2020. Association for Computing Machinery.

[50] Xilinx Inc. *XC2C64A CoolRunner-II CPLD.* Version 2.3.

[51] G. Yang and Y. Liang. Backscatter communications over ambient ofdm signals: Transceiver design and performance analysis. In *2016 IEEE Global Communications Conference (GLOBECOM)*, pages 1–6, Dec 2016.

[52] Yu Ge, Jeng Wai Kwan, J. S. Pathmasuntharam, Zhengye Di, T. S. P. See, Wei Ni, Chee Wee Kim, Tat Meng Chiam, and Maode Ma. Performance benchmarking for wireless body area networks at 2.4 ghz. In *2011 IEEE 22nd International Symposium on Personal, Indoor and Mobile Radio Communications*, pages 2249–2253, 2011.

[53] P. Zhang, D. Bharadia, K. Joshi, and S. Katti. Enabling backscatter communication among commodity wifi radios. In *Proceedings of the 2016 conference on ACM SIGCOMM 2016 Conference*, pages 611–612. ACM, 2016.

[54] P. ZHANG, D. Bharadia, K. Joshi, and S. Katti. Enabling backscatter communication among commodity wifi radios. In *Proceedings of the 2016 ACM SIGCOMM Conference*, SIGCOMM '16, pages 611–612, New York, NY, USA, 2016. ACM.

[55] P. Zhang, D. Bharadia, K. R. Joshi, and S. Katti. Hitchhike: Practical backscatter using commodity wifi. In *SenSys*, pages 259–271, 2016.

[56] P. Zhang, C. Josephson, D. Bharadia, and S. Katti. Freerider: Backscatter communication using commodity radios. In *Proceedings of the 13th International Conference on Emerging Networking EXperiments and Technologies*, CoNEXT '17,

2017.

[57] P. ZHANG, M. Rostami, P. Hu, and D. Ganesan. Enabling practical backscatter communication for on-body sensors. In *Proceedings of the 2016 ACM SIGCOMM Conference*, SIGCOMM '16, pages 370–383, New York, NY, USA, 2016. ACM.

[58] R. Zhao, F. Zhu, Y. Feng, S. Peng, X. Tian, H. Yu, and X. Wang. Ofdma-enabled wi-fi backscatter. In *The 25th Annual International Conference on Mobile Computing and Networking*, MobiCom '19, New York, NY, USA, 2019. Association for Computing Machinery.